Med Chem Res (2013) 22:4663–4676
DOI 10.1007/s00044-012-0461-8

MEDICINAL CHEMISTRY RESEARCH

ORIGINAL RESEARCH

Synthesis, structure, anticancer, and antioxidant activity of *para*-xylyl linked bis-benzimidazolium salts and respective dinuclear Ag(I) *N*-heterocyclic carbene complexes (Part-II)

Rosenani A. Haque · Muhammad Adnan Iqbal · Patrick Asekunowo · A. M. S. Abdul Majid · Mohamed B. Khadeer Ahamed · Muhammad Ihtisham Umar · Sawsan S. Al-Rawi · Fouad Saleih R. Al-Suede

Received: 1 November 2012 / Accepted: 28 December 2012 / Published online: 18 January 2013

Abstract The article describes synthesis, characterization (NMR, FT-IR, microanalysis, X-ray crystallography), in vitro anticancer, and antioxidant activity of *para*-xylyl linked bis-benzimidazolium salts and respective dinuclear Ag–NHC complexes. All the compounds were tested for their cytotoxicity against human colorectal cancer cells (HCT 116) and DPPH antioxidant evaluation. According to cell viability measurements using MTT assay, all the tested compounds showed dose-dependent cytotoxic activity against HCT 116 cells. The tested compounds demonstrated significant activity with IC_{50} values range 0.29–3.30 μM for HCT 116 and % age inhibition 6.37–21.00 for DPPH antioxidant study. 5-Fluorouracil was used as standard drug (IC_{50} 19.2 μM for HCT 116) whereas for DPPH analysis, Gallic acid was used as positive control (% age inhibition 77.68). All the compounds showed potential anticancer activity against human colorectal cancer whereas antioxidant activity was not significant. We found that as the size of *N*-alkyl substitution on benzimidazolium salt increases its cytotoxicity against cancer decreases whereas a reverse occurs in case of respective complexes.

Keywords Benzimidazole · Benzimidazolium salts · *N*-Heterocyclic carbenes (NHCs) · Ag–NHC complexes · Human colon cancer (HCT 116) · Antioxidant

Introduction

Recently, we reported that *para*-xylyl linked bis-benzimidazolium salts (halides/PF_6) and respective dinuclear Ag(I)–NHC complexes are potentially active against Human Colon Cancer (HCT 116) and Leukemia (HL-60) (Iqbal *et al.,* 2013). We also mentioned that bis-benzimidazolium chlorides are many fold active over similar bis-benzimidazolium hexaflourophosphate (PF_6) salts. This is also in accordance with our previous report where we first time pointed out the significance of halides over hexafluorophosphate as counter anions for *meta*-xylyl linked bis-benzimidazolium salts (Haque *et al.,* 2012e). In view of our previous results, all the current *para*-xylyl linked bis-benzimidazolium salts (ligands) were synthesized and applied on cancer cells keeping bromide as counter anions. However, in part-I of this article, we used chloride instead of bromide. Also, we discussed that as the size (chain length) of *N*-substitution increases the activity of ligands decreases whereas a reverse occurs in case of respective dinuclear complexes. In general, almost all the Ag(I)-NHC complexes were found to be more active compared to respective ligands. The current results further support our

Electronic supplementary material The online version of this article (doi:10.1007/s00044-012-0461-8) contains supplementary material, which is available to authorized users.

R. A. Haque (✉) · M. A. Iqbal (✉) · P. Asekunowo
The School of Chemical Sciences, Universiti Sains Malaysia, 11800 USM Penang, Malaysia
e-mail: rosenani@usm.my

M. A. Iqbal
e-mail: mai10_che022p@student.usm.my; adnan_chem38@yahoo.com

A. M. S. A. Majid · M. B. Khadeer Ahamed · S. S. Al-Rawi · F. S. R. Al-Suede
EMAN Research and Testing Laboratory, The School of Pharmaceutical Sciences, Universiti Sains Malaysia, 11800 USM Penang, Malaysia

M. I. Umar
The School of Pharmaceutical Sciences, Universiti Sains Malaysia, 11800 USM Penang, Malaysia

previous findings. Previously we used ethyl, propyl, and butyl as *N*-substitutions and in this article we used octyl, nonyl, and decyl as *N*-substitutions.

Human Colorectal Cancer/tumor (HCT) is the third most common cancer and the fourth most frequent cause of cancer deaths worldwide (Weitz *et al.,* 2005). According to an estimate, every year more than 945,000 people develop this cancer and around 492,000 patients die (Weitz *et al.,* 2005). This cancer is caused by uncontrolled cell growth in the colon, rectum, or vermiform appendix and is more common in older age males. The major reasons of this cancer are: diet poor in fiber, folate, and calcium or rich in meat and fat, smoking and high alcohol intake (Weitz *et al.,* 2005). Benzimidazole is a heterocyclic moiety possessing a wide spectrum of biological activities; a number of its organic derivatives have shown potential anticancer activity against Leukemia (HL-60), Breast Cancer (MCF-7), Human colon adenocarcinoma (HT-29), and Cervical cancer (HeLa) (Narasimhan *et al.,* 2012) including a number of other therapeutic activities (Bansal and Silakari, 2012). Due to the aforementioned reasons, a number of benzimidazolium salts (organic salts, **IV–VI**) were synthesized, unlike organic derivatives of benzimidazole (organic compounds), in order to increase the solubility and efficacy of these heterocycles. Furthermore, each organic salt was bonded with silver metal ions through carbene carbon (metal complexes, **VII–IX**) to further assess its medicinal efficacy.

Experimental

Reagents and instruments

Nuclear magnetic resonance spectra were recorded on Bruker 500 MHz Ultrashield^{TM} spectrometer at ambient temperature. ^{1}H and ^{13}C NMR peaks are labeled as singlet (s), doublet (d), triplet (t), and multiplet (m); Chemical shifts were referenced with respect to solvent signals. FT-IR spectra were recorded on Perkin Elmer-2000. Elemental analysis was carried out on a Perkin Elmer series II, 2400 microanalyzer. X-ray diffraction data were taken with Bruker SMART APEX2 CCD area-detector diffractometer. The melting and boiling points were assessed using a Stuart Scientific SMP-1 (UK) instrument. Chemicals and solvents were used as received without further purifications.

RPMI 1640 was purchased from ScienCell, USA. Trypsin and heat inactivated fetal bovine serum (HIFBS) were obtained from GIBCO, UK. Phosphate buffered saline (PBS), penicillin/streptomycin (PS) solution, MTT reagent, and 5-fluorouracil were purchased from Sigma-Aldrich, Germany. All other chemicals used in this study were analytical grade or better.

Cell lines and culture conditions

Human colorectal tumor (HCT 116) cell line was purchased from American type culture collection (Rockvill, MD, USA). HCT 116 cell line has been derived from colonic epithelial carcinoma. The cells were maintained in RPMI 1640 containing 10 % HIFBS and 1 % PS. Cells were cultured in 5 % CO_2-humidified atmosphere at 37 °C.

Synthesis of *N*-substituted-bis-benzimidazolium salts (**I–III**): general procedure

All *N*-alkyl benzimidazole compounds were prepared according to the literature (Starikova *et al.,* 2003) method with slight modifications. In general, potassium hydroxide (1.5 equiv.) was added to a solution of benzimidazole (1 equiv.) in DMSO (30–40 ml for 0.01–0.02 M of reactants), and mixture was stirred for 30 min at RT (25–27 °C), and respective alkyl halide (1 equiv.) was added dropwise under vigorous stirring. After 2 h, the mixture was poured into 200–300 ml of water and extracted with chloroform (6 × 25 ml), the combined extract was filtered through five plies of Whatman filter papers in order to dry the extract. This process of filtration was repeated twice to collect crystal clear solution of desired compound which was finally evaporated under reduced pressure. See Supplementary 1 file for diagrammatic illustration of work up process. Desired compounds were obtained either as thick yellowish or colorless fluids and characterized by spectroscopic (FT-IR and NMR) techniques and compared with literature before further use (Haque and Iqbal, 2012b).

Synthesis of *N*-substituted-bis-benzimidazolium salts (**IV–VI**): general procedure

Respective *N*-substituted benzimidazole (2 equiv.) was added dropwise in a vigorously stirring solution of 1,4-bis(bromomethylene)benzene (1 equiv.) in 30–40 ml of 1,4-dioxane and refluxed for 24 h. All the salts appeared as solid (precipitates) in the reaction medium. The precipitates were collected, washed with fresh 1,4-dioxane (3 × 5 ml), dried at RT for 24 h, and ground to fine powder (see Supplementary 2).

*Synthesis of 3,3′-(1,4-phenylenebis(methylene))bis(1-octylbenzimidazolium) dibromide (**IV**.2Br)*

Following the general procedure, *N*-octylbenzimidazole (**I**) 20 mM (4.60 g) and 1,4-bis(bromomethylene)benzene 10 mM (2.63 g); the product appeared as white lumps, filtered, washed with fresh 1,4-dioxane (3 × 5 ml), and dried at RT. The product was collected as crunchy lumps. White powder; yield: 79.92 % (5.77 g); mp 226–228 °C.

FT-IR (KBr, ν_{max}, cm^{-1}): 3,401 (C_{aliph}–$N_{benzimi}$); 3124, 3059, 3028 (C–H_{arom}); 2961, 2855 (C–H_{aliph}); 1342, 1377, 1422, 1455, 1478 (C_{arom}–$N_{benzimi}$). ^{1}H NMR (500 MHz, DMSO-d_6): $\delta = 0.82$ (6H, t, 2× CH_3, $J = 7.5$ Hz), 1.14–1.35 (20H, br.m, 10× CH_2), 1.92 (4H, pent., 2× CH_2, $J = 7.5$ Hz), 4.52 (4H, t, 2× N–CH_2–R, $J = 7.5$ Hz), 5.83 (4H, s, 2× N–CH_2–Ar), 7.60 (4H, s, Ar–H), 7.65 (4H, sext, Ar–H), 7.98 (2H, d, Ar–H, $J = 8.0$ Hz), 8.12 (4H, d, Ar–H, $J = 8.0$ Hz), 10.24 (2H, s, 2 × NCHN). ^{13}C NMR (125 MHz, DMSO-d_6): $\delta = 13.8$ (CH_3), 21.9, 25.7 (CH_2), 28.3 ($J_{C4/5} = 13.9$ Hz, $J_{C5/6} = 2.5$ Hz,), 31.0 (CH_2), 46.8 (N–CH_2–R), 49.3 (N–CH_2–Ar), 113.8 (d, Ar–C, $J = 11.2$ Hz), 126.6 ($J = 2.5$ Hz), 128.8, 130.7, 131.2, 134.5 (Ar–C), 142.3 (NCHN). Anal. Calcd for $C_{38}H_{52}Br_2N_4$: C, 62.98; H, 7.23; N, 7.73. Found: C, 62.82; H, 7.18; N, 7.51.

*Synthesis of 3,3′-(1,4-phenylenebis(methylene))bis(1-nonyl-benzimidazolium) dibromide (**V**.2Br)*

Following the general procedure, *N*-nonylbenzimidazole (**II**) 20 mM (4.88 g) and 1,4-bis(bromomethylene)benzene 10 mM (2.63 g); the product appeared as shiny white precipitates in light yellow reaction medium, filtered, washed with fresh 1,4-dioxane (3 × 5 ml), and dried at RT. The product was collected as soft lumps. White powder; yield: 97.07 % (7.30 g); mp 224-226 °C. FT-IR (KBr, ν_{max}, cm^{-1}): 3415, 3367 (C_{aliph}–$N_{benzimi}$), 3122, 3030 (C–H_{arom}), 2955, 2921, 2849 (C–H_{aliph}), 1341, 1379, 1422, 1451, 1479 cm^{-1} (C_{arom}–$N_{benzimi}$). ^{1}H NMR (500 MHz, DMSO-d_6): $\delta = 0.82$ (6H, t, 2× CH_3, $J = 7.0$ Hz), 1.20–1.34 (20H, two br.ds, 10× CH_2), 1.92 (4H, pent., 2× CH_2, $J = 7.5$ Hz), 4.52 (4H, t, 2× N–CH_2–R, $J = 7.5$ Hz), 5.83 (4H, s, 2× N–CH_2–Ar), 7.61 (4H, s, Ar–H), 7.63 (4H, sext, Ar–H), 7.98 (2H, d, Ar–H, $J = 8.0$ Hz), 8.12 (4H, d, Ar–H, $J = 8.0$ Hz), 10.25 (2H, s, 2× NCHN). ^{13}C NMR (125 MHz, DMSO-d_6): $\delta = 13.7$ (CH_3), 21.9, 25.6 (CH_2), 28.3, 28.3, 28,4, 28.6 ($J_{C4/5} = 1.2$ Hz, $J_{C5/6} = 12.5$ Hz, $J_{C6/7} = 27.5$ Hz), 31.0 (CH_2), 46.7 (N–CH_2–R), 49.2 (N–CH_2–Ar), 113.8 (d, Ar–C, $J = 8.7$ Hz), 125.1 (Ar–C), 126.5 ($J = 3.7$ Hz), 128.8, 130.6, 131.1, 134.4 (Ar–C), 142.3 (NCHN). Anal. Calcd for $C_{40}H_{56}Br_2N_4$: C, 63.83; H, 7.50; N, 7.44. Found: C, 63.82; H, 7.48; N, 7.41.

*Synthesis of 3,3′-(1,4-phenylenebis(methylene))bis(1-decyl-benzimidazolium) dibromide (**VI**.2Br)*

Following the general procedure, *N*-decylbenzimidazole (**III**) 20 mM (5.16 g) and 1,4-bis(bromomethylene)benzene 10 mM (2.63 g); the product appeared as shiny white crystalline powder in light yellow reaction medium, filtered, washed with fresh 1,4-dioxane (3 × 5 ml), and dried at RT. The product was collected as crystalline powder. White crystalline powder; yield: 78.02 % (6.07 g); mp 214–216 °C. FT-IR (KBr, ν_{max}, cm^{-1}): 3416 (C_{aliph}–$N_{benzimi}$); 3123, 3032 (C–H_{arom}); 2952, 2922, 2852 (C–H_{aliph}); 1343, 1375, 1422, 1451, 1476 (C_{arom}–$N_{benzimi}$). ^{1}H NMR (500 MHz, DMSO-d_6): $\delta = 0.82$ (6H, t, 2 × CH_3, $J = 7.0$ Hz), 1.20–1.30 (32H, two br.d, 16× CH_2), 1.91 (4H, pent., 2× CH_2, $J = 7.5$ Hz), 4.52 (4H, t, 2× N–CH_2–R, $J = 7.5$ Hz), 5.82 (4H, s, 2× N–CH_2–Ar), 7.59 (4H, s, Ar–H), 7.63 (4H, sext, Ar–H), 7.96 (2H, d, Ar–H, $J = 8.0$ Hz), 8.10 (4H, d, Ar–H, $J = 8.0$ Hz), 10.21 (2H, s, 2 × NCHN). ^{13}C NMR (125 MHz, DMSO-d_6): $\delta = 13.8$ (CH_3), 21.9, 25.6 (CH_2), 28.3, 28.5, 28.7, 28.7 ($J_{C4/5} = 23.7$ Hz, $J_{C5/6} = 22.5$ Hz, $J_{C6/7} = 6.2$ Hz), 31.1 (CH_2), 46.7 (N–CH_2–R), 49.2 (N–CH_2–Ar), 113.8 0(d, Ar–C, $J = 7.5$ Hz), (Ar–C), 126.5 ($J = 2.5$ Hz), 128.8, 130.6, 131.2, 134.5 (Ar–C), 142.3 (NCHN). Anal. Calcd for $C_{42}H_{60}Br_2N_4$: C, 64.61; H, 7.75; N, 7.18. Found: C, 64.63; H, 7.68; N, 7.11.

Synthesis of Ag(I)–NHC complexes (**VII–IX**): general procedure

In general, respective bis-benzimidazolium salt (**IV–VI**.2Br; 2 equiv.) was dissolved in MeOH (70–80 ml) along with silver oxide (1 equiv.) and the mixture was stirred for two days at room temperature. For each reaction RB flask was covered by aluminum foil to stop the interaction of light with reaction mixture. The reaction mixture was filtered through Celite (545) to get crystal clear solution. In a separate RB flask KPF_6 (2.5 equiv.) was dissolved in MeOH (30–40 ml), filtered, and was added slowly in previously obtained solution of complex. The solution was stirred for 3 h. The precipitates so obtained were filtered and washed by water (3 × 5 ml) and MeOH (3 × 5 ml). The PF_6 salt of each complex was dried at RT for several days and ground to fine powder (see supplementary 3). The color, state, mp, and characterization is described under each heading.

*Synthesis of 1,4-bis(N-octylbenzimidazol-1ylmethyl)benzene-silver(I) bis(hexaflourophosphate) complex (**VII**)*

Following the general procedure, **IV**.2Br, 3.4 mM (2.50 g) and silver oxide, 7.0 mM (1.60 g). light gray soft powder; yield: 84.47 % (2.34 g); mp 262–264 °C. FT-IR (KBr, ν_{max}, cm^{-1}): 3434 (C_{aliph}–$N_{benzimi}$); 3110, 3060 (C–H_{arom}); 2953, 2927, 2854 (C–H_{aliph}); 1356, 1401, 1445, 1478 (C_{arom}–$N_{benzimi}$). ^{1}H NMR (500 MHz, DMSO-d_6): $\delta = 0.65$ (12H, t, 4× CH_3, $J = 7.0$ Hz), 1.05 (16H, br.m, 6× CH_2), 1.13 (8H, pent., 4× CH_2), 1.23 (8H, pent., 4× CH_2), 1.33 (8H, pent.,4× CH_2),1.91 (8H, pent.,

4× CH_2), 4.59 (8H, t, 4× N–CH_2–R, $J = 6.5$ Hz), 5.74 (8H, s, 4× N–CH_2–Ar), 7.21 (8H, s, Ar–H), 7.38–7.46 (8H, sext., Ar–H), 7.76 (4H, d, Ar–H, $J = 8.0$ Hz), 7.86 (4H, d, Ar–H, $J = 8.0$ Hz). ^{13}C NMR (125.1 MHz, DMSO-d_6): $\delta = 13.7$ (CH_3), 21.8, 26.2, 28.4 (d, $J = 17.5$ Hz), 30.0, 31.5 (alkyl chain 6× CH_2), 48.6 (N–CH_2–R), 51.1 (N–CH_2–Ar), 112.2, 124.2, 127.3 (Ar–C), 133.3 (d, Ar–C, $J = 16.2$ Hz), 136.1 (Ar–C), 187.4 and 189.2 (br.d, $^1J_{(C–Ag)} = 192$ Hz). Anal. Calcd for $C_{76}H_{104}Ag_2N_8P_2$: C, 55.82; H, 6.41; N, 6.85. Found: C, 55.57; H, 6.61; N, 6.79.

*Synthesis of 1,4-bis(N-nonylbenzimidazol-1ylmethyl)benzene-silver(I) bis(hexaflourophosphate) complex (**VIII**)*

Following the general procedure, **V**.2Br, 4.0 mM (3.0 g) and silver oxide, 7.0 mM (1.60 g). dark gray powder; yield: 67.65 % (2.28 g); mp 274–276 °C. FT-IR (KBr, ν_{max}, cm^{-1}): 3,437 (C_{aliph}–$N_{benzimi}$); 3,110, 3,063, 3,039 (C–H_{arom}); 2,954, 2,925, 2,854 (C–H_{aliph}); 1,350, 1,401, 1,444, 1,480 (C_{arom}–$N_{benzimi}$). ^{1}H NMR (500 MHz, DMSO-d_6): $\delta = 0.68$ (12H, t, 4× CH_3, $J = 7.0$ Hz), 1.06 (32H, br.m, 16× CH_2), 1.23 (8H, pent., 4× CH_2), 1.33 (8H, pent., 4× CH_2),1.90 (8H, pent., 4× CH_2), 4.58 (8H, t, 4× N–CH_2–R, $J = 6.5$ Hz), 5.73 (8H, s, 4× N–CH_2–Ar), 7.19 (8H, s, Ar–H), 7.38–7.45 (8H, sext., Ar–H), 7.75 (4H, d, Ar–H, $J = 8.0$ Hz), 7.85 (4H, d, Ar–H, $J = 8.0$ Hz). ^{13}C NMR (125.1 MHz, DMSO-d_6): $\delta = 13.7$ (CH_3), 21.9, 26.2, 28.6 ($t_{C4.C5.C6}$, $J_{C4.C5} = 20.0$ Hz, $J_{C5.C6} = 15.0$ Hz), 30.0, 31.5 (alkyl chain 7× CH_2), 48.68 (N–CH_2–R), 51.1 (N–CH_2–Ar), 112.2 (d, Ar–C, $J = 2.5$ Hz), 124.2, 127.3 (Ar–C), 133.3 (d, Ar–C, $J = 15.0$ Hz), 136.1 (Ar–C), 187.7 and 189.3 [d, $^1J_{(C\text{-}109Ag)} = 208$ Hz] & [*d*, $^1J_{(C\text{-}107Ag)} = 181$ Hz]. Anal. Calcd for $C_{80}H_{112}Ag_2N_8P_2$: C, 56.81; H, 6.67; N, 6.62. Found: C, 56.57; H, 6.61; N, 6.56.

*Synthesis of 1,4-bis(N-decylbenzimidazol-1ylmethyl)benzene-silver(I) bis(hexaflourophosphate) complex (**IX**)*

Following the general procedure, **VI**.2Br, 3.2 mM (2.50 g) and silver oxide, 6.4 mM (1.48 g). Light pink shiny powder; yield:7 6.97 % (2.78 g); mp 258–260 °C. FT-IR (KBr, ν_{max}, cm^{-1}): 3,437 (C_{aliph}–$N_{benzimi}$); 3,108, 3,061 (C-H_{arom}); 2,922, 2,853 (C–H_{aliph}); 1,345, 1,399, 1,466, 1,479 (C_{arom}–$N_{benzimi}$). ^{1}H NMR (500 MHz, DMSO-d_6): $\delta = 0.69$ (12H, *t*, 4× CH_3, $J = 7.0$ Hz), 1.06 (40H, br.m, 20× CH_2), 1.23 (8H, pent., 4× CH_2), 1.34 (8H, pent., 4× CH_2),1.90 (8H, pent., 4× CH_2), 4.59 (8H, t, 4× N–CH_2–R, $J = 6.5$ Hz), 5.74 (8H, *s*, 4× N–CH_2–Ar), 7.21 (8H, *s*, Ar–H), 7.38–7.45 (8H, sext., Ar–H), 7.76 (4H, *d*, Ar–H, $J = 2.0$ Hz), 7.85 (4H, *d*, Ar–H, $J = 2.0$ Hz). ^{13}C NMR (125.1 MHz, DMSO-d_6): $\delta = 13.7$ (CH_3), 21.9, 26.2, 28.6 ($t_{C4.C5.C6}$, $J_{C4.C5} = 15.0$ Hz, $J_{C5.C6} = 20.0$ Hz), 30.0, 31.1 (alkyl chain 8× CH_2), 48.6 (N–CH_2–R), 51.1 (N–CH_2–Ar), 112.2 (d, Ar–C, $J = 12.5$ Hz), 124.2 (d, Ar–C, $J = 3.7$ Hz), 127.3 (Ar–C), 133.3 (d. d, Ar–C, $J = 16.2$ Hz and $J = 10.0$ Hz), 136.13 (Ar–C), 187.7 and 189.3 [d, $^1J_{(C\text{-}109Ag)} = 208$ Hz] and [d, $^1J_{(C\text{-}107Ag)} = 181$ Hz]. Anal. Calcd for $C_{84}H_{120}Ag_2N_8P_2$: C, 57.73; H, 6.92; N, 6.41. Found: C, 57.70; H, 6.82; N, 6.32.

In vitro anticancer activity

Preparation of cell culture

Initially, human colorectal carcinoma (HCT 116) cell line was allowed to grow under optimal incubator conditions. Cells that have reached a confluence of 70–80 % were chosen for cell plating purposes. Old medium was aspirated out of the flask. Next, cells were washed using sterile phosphate buffered saline (PBS) (pH 7.4), 2–3 times. PBS was completely discarded after washing. Following this, trypsin was added and distributed evenly onto cell surfaces. Cells were incubated at 37 °C in 5 % CO_2 for 1 min. Then, the flasks containing the cells were gently tapped to aid cells segregation and observed under inverted microscope. Trypsin activity was inhibited by adding 5 ml fresh media (10 % FBS). Cells were counted and diluted to get a final concentration of 2.5×10^5 cells/ml, and inoculated into wells (100 µl cells/well). Finally, plates containing the cells were incubated at 37 °C with an internal atmosphere of 5 % CO_2.

MTT assay

Cancer cells (100 µl, 1.5×10^5 cells/ml) were inoculated in 96-well microtiter plate. Then the plate is incubated in CO_2 incubator for overnight in order to allow the cells for attachment. 100 µl of test substance was added into each well containing the cells. Test substance was diluted with media into the desired concentrations from the stock. The plates were incubated at 37 °C with an internal atmosphere of 5 % CO_2. After 48 h treatment period, 20 µl of MTT reagent was added into each well and incubated again for 4 h. After this incubation period, 50 µl of MTT lysis solution (DMSO) was added into each well. The plates were further incubated for 5 min in CO_2 incubator. Finally, plates were read at 570 and 620 nm wavelengths using a monochromator based multimode microplate reader (Tecan Infinite® M1000 PRO). Data were recorded and analyzed for the assessment of the effects of test substance on cell viability and growth inhibition. The percentage of growth inhibition was calculated from the optical density (OD) that was obtained from MTT assay.

Antioxidant activity

Materials and methods

The antioxidant potential of the compounds **IV–IX** and benzimidazole (**X**) was assessed by evaluating the hydrogen–donating ability of the compounds in the presence of DPPH (2,2-diphenyl-1-picrylhydrazyl) stable radical according to the reported method (Kim *et al.,* 2003) with minor modifications. The samples and Gallic acid (positive control) were dissolved in DMSO to make five concentrations i.e., 400, 200, 100, 50, and 25 µM. 100 µl of 0.008 % DPPH solution in methanol was added in each well of 96-well plate followed by the addition of 100 µl of the sample solution. The wells with 100 µl of DPPH solution and DMSO were taken as negative control wells. The plate was incubated at 37 °C for 30 min. Absorbance of the methanolic DPPH-tincture was measured at 517 nm using microplate reader (Tecan Infinite® M1000 PRO). The % inhibition of free radical scavenging activity was calculated using the following formula:

$$\%\,\text{Inhibition} = [1-(A/B)] \times 100$$

where, *A* is the OD of the treatment well and *B* is the OD of the control well.

Results and discussion

Benzimidazole is a medicinally important heterocyclic moiety (Narasimhan *et al.,* 2012) where its derivatives are structural isostere of naturally occurring nucleotides which allow them to interact with the biopolymers of living systems. It was, therefore, of great interest to investigate the bis-benzimidazolium salts and respective dinuclear Ag(I)–NHC complexes against various types of cancers.

Synthesis

The reaction of two equivalents of *N*-alkylbenzimidazole with 1,4-bis(bromomethylene)benzene in 1,4-dioxane at 100 °C for 24 h afforded the *para*-xylyl linked bis-benzimidazolium salts (**IV–VI**) with 78–97 % yield. We have already reported the synthesis and structure of a number of *ortho*-xylyl linked bis-benzimidazolium salts (Haque and Iqbal, 2012b, 2012a; Haque *et al.,* 2012c, 2012d, 2011, 2012f). The use of 1,4-dioxane as a reaction medium for the synthesis of bis-benzimidazolium salts is highly recommended because of its moderate polarity and suitable boiling point (101 °C). Using 1,4-dioxane as a reaction medium, bis-benzimidazolium salts can be collected either directly as a solid from reaction medium using common filtration method or by decantation when a salt settles as a thick yellowish fluid at the bottom of the flask (see Supplementary 2). The solubility of these salts in 1,4-dioxane increases with increase in chain length. We observed this phenomenon in case of *ortho*-xylyl linked bis-benzimidazolium halides where *N*-ethyl substituted *ortho*-xylyl linked bis-benzimidazolium bromide was completely insoluble even in hot 1,4-dioxane but *N*-decyl substituted one was completely soluble under the same conditions and reaction mixture had to cool down to room temperature (overnight) to collect it as a crystalline powder (Haque and Iqbal, 2012b). In case of *para*-xylyl linked bis-benzimidazolium halides, all the salts (ethyl-decyl *N*-substituted) were completely insoluble even in hot 1,4-dioxane. However, all the xylyl (*ortho*/*meta*/*para*) linked bis-benzimidazolium salts in halide form are soluble in polar solvents like methanol, ethanol, DMSO, and DMF; and insoluble in common non-polar to slightly polar solvents like benzene, diethyl ether, *n*-hexane, toluene, etc. The synthesis of bis-benzimidazolium salts can also be carried out in other solvents like methanol, ethanol, acetonitrile, etc. but collection of bis-benzimidazolium salts as halides in pure form becomes difficult and counter anion conversion to PF_6 by metathesis route becomes compulsory to achieve the purity.

Synthesis of dinuclear Ag–NHC (**VII–IX**) complexes using azolium halides as a starting material is of significance importance, because using this method pure form of desired complex can be obtained with ease. Scheme 1 shows three simple steps for the synthesis, starting from *N*-alkylated benzimidazoles to PF_6 salts of dinuclear Ag–NHC complexes (see Supplementary 3).

FT-IR spectra of the compounds

The bis-benzimidazolium halides do not have many functional groups to be characterized by FT-IR spectroscopic technique but it is possible to study the spectral features of ligands (**IV–VI**) and respective Ag(I)–NHC (**VII–IX**) complexes in both near and mid IR spectra as specific patterns can be observed which may be used as primary indicators of a successful synthesis (Iqbal *et al.,* 2013).

For ligands (**IV–VI**.2Br), strong and sharp stretching vibrations (3,406–3,415 cm^{-1}) appeared for tertiary nitrogens of benzimidazolium ring (C_{aliph}–$N_{benzimi}$) which are usually overlapped by water peak due to the presence of water in these compounds (see Fig. 1). In single crystal structures of these bis-benzimidazolium halides these water molecules are found to be attached with halide (X = Cl/Br) anions through X–H–O hydrogen bondings (Haque *et al.,* 2012b, 2012d, 2011; Iqbal *et al.,* 2013). The pure modes of the C_{sp3}–H stretching vibrational bands in both, alkyl benzimidazoles and bis-benzimidazolium salts appeared at around 2,900–3,000 cm^{-1} ($C–H_{aliph}$). This variation in the

Step-I

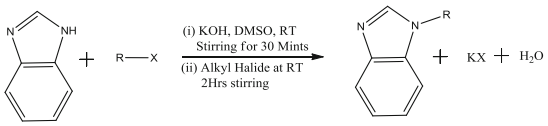

I (R = Octyl), **II** (Nonyl), **III** (Decyl),
X = Br

Step II

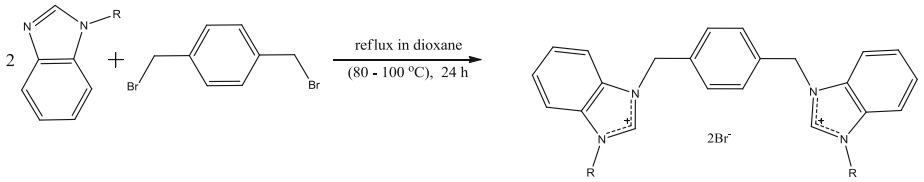

IV (R = Octyl), **V** (Nonyl), **VI** (Decyl)

Step III

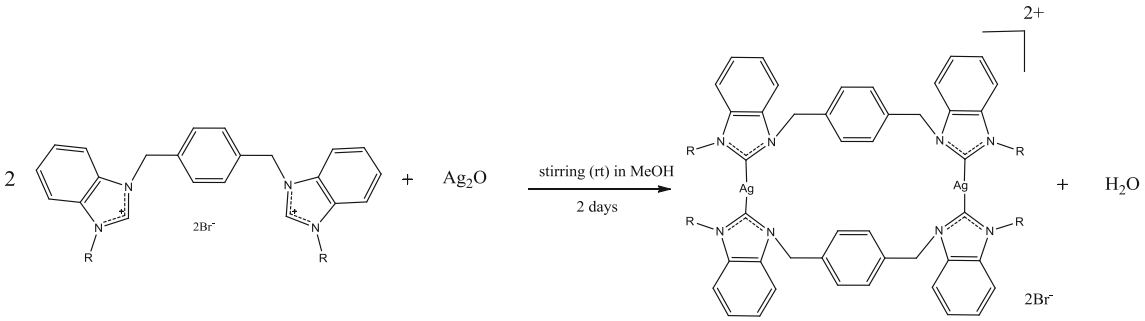

VII' - IX'. 2Br

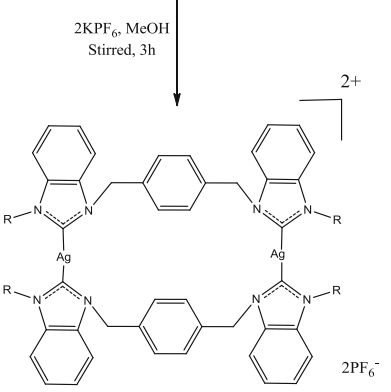

VII - IX. $2PF_6$

VII (R = Octyl), **VIII** (Nonyl), **IX** (Decyl)

Scheme 1 Synthesis of *N*-alkyl benzimidazoles (**I–III**), 3,3′-(1,4-phenylenebis(methylene))bis(1-alkyl-Benzimidazolium) salts (**IV–VI**), and Ag–NHC complexes (**VII–IX**)

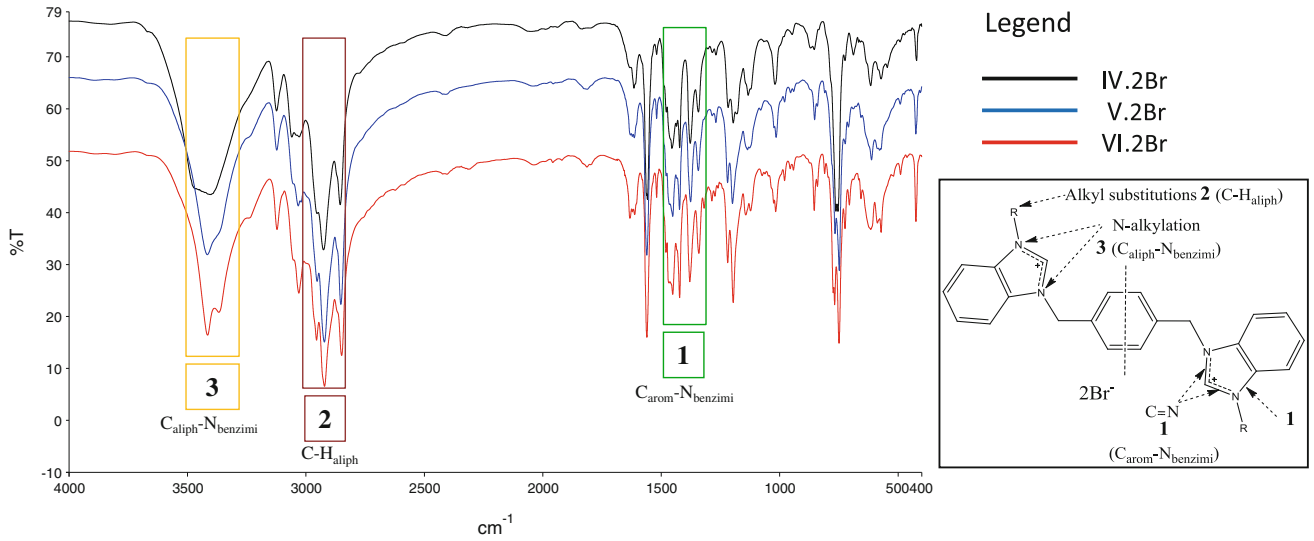

Fig. 1 FT-IR spectra (Overlay) of *para*-xylyl linked bis-benzimidazolium salts (**IV–VI**.2Br) highlighting C_{aliph}–$N_{benzimi}$ stretching (*3*), C–H_{aliph} stretching (*2*), & C_{arom}–$N_{benzimi}$ (*1*). The *figure* shows overlap of pure modes of tertiary amine (*3*) by hydrated water molecule. See part-I of this article for pure modes (Iqbal *et al.,* 2013)

range is due to the presence of C–H (sp^3-s) stretching of alkyl chains and methylene (N–CH_2–Ar) group. This can be further classified as the vibrational bands in the range 2,848–2,856 cm^{-1} appeared for CH_3 stretchings, 2,920–2,925 cm^{-1} for CH_2 anti-symmetric stretchings, and 2,953–2,958 cm^{-1} for CH_2 symmetric stretchings (see Supplementary 4). A strong and sharp intense band was observed in the range 1,350–1,500 cm^{-1} ascribed to the stretching modes of vibrations of benzimidazole ring due to the presence of–HC=N–module (Iqbal *et al.,* 2013; Hranjec *et al.,* 2011). The reduction in the intensity of this band in ligands (**IV–VI**.2Br) as compared to respective *N*-alkyl-benzimidazoles is probably caused by the conjugation of of C = N bond with the benzimidazole ring and due to *N*-alkylation, where alkyl groups act as electron donating entities. The other ring vibrations are intense bands at around 1,050 and 1,220 cm^{-1}.

As described earlier (Iqbal *et al.,* 2013), we found some interesting features of FT-IR to confirm a successful synthesis of Ag(I)–NHC complexes. We observed that bonding of NHC carbon with silver metal ion strengthens vibrations in the range 1,350–1,500 cm^{-1} and a characteristic "four

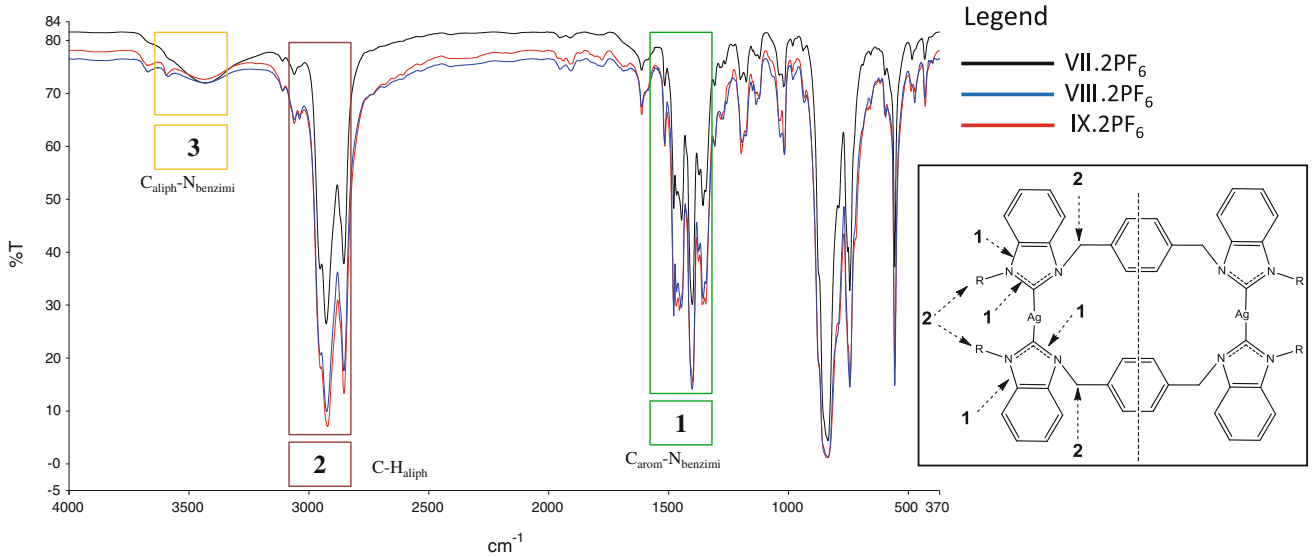

Fig. 2 FT-IR spectra (Overlay) of Ag–NHC complexes (**VII–IX**.$2PF_6$) highlighting C_{arom}–$N_{benzimi}$ stretch (*1*) after successful reaction. The *figure* shows that a "*four fingers (f.fs.)*" pattern appears on FT-IR spectrum for each Ag–NHC complex. This information can be used as primary confirmation

Table 1 IC_{50} values of tested samples against HCT 116 cell line and % age inhibition values for DPPH alanysis

Compound	*R*	Compounds	IC $_{50}$ (μM) HCT 116	% DPPH
Ligands	Octyl	**IV**	0.9	17.91
	Nonyl	**V**	2.8	14.84
	Decyl	**VI**	3.3	13.66
Ag(I)–NHC complexes	Octyl	**VII**	2.2	7.40
	Nonyl	**VIII**	0.29	6.37
	Decyl	**IX**	1.2	9.27
Benzimidazole (starting material)	–	**X**	>200	21.00
Standard drug		5-FU	19.2	–
		Gallic acid	–	77.68

fingers *(f.fs)*" pattern appears for the Ag(I)–NHC complexes. This region is specific for –C=N (C_{arom}–$N_{benzimi}$) and CH_2 bending vibrations. The observed "f.fs" pattern is entirely different than all the respective vibrations in azolium salts and is easily distinguishable (See Fig. 2). This information can be used as primary confirmation of desired Ag(I)–NHC complex.

FT-NMR spectra of the compounds

FT-NMR spectra of all the compounds were analyzed in DMSO-d_6 over the scan range 0–16 δ ppm for ^{1}H NMR and 0–200 δ ppm for ^{13}C NMR studies. ^{1}H NMR spectra of all the salts (**IV**–**VI**) evidenced a sharp singlet in the range 10.21–10.25 δ ppm ascribed to the benzimidazolium ring (NCHN) acidic proton. These signals are in accordance with previous reports (Haque and Iqbal, 2012a, b). Synthesis of Ag–NHC complexes was confirmed by the disappearance of acidic proton peak "Hc" and notice of observable changes in benzylic peaks (see Supplementary 5*)*. The methylene (N–CH_2–Ar) group, which connects *para*-xylyl unit with benzimidazolium units, displays a sharp singlet at 5.83 δ ppm. Finally, the resonance of *N*-substituted alkyl chain protons appeared in the range 0.8–4.5 δ ppm. Similarly, the structural features of the salts were further confirmed by the ^{13}C NMR data. The spectra of all the salts displayed a distinguished peak in the most down field region at 142.3 δ ppm ascribed to the benzimidazole ring carbon (NCN). The signals for methylene (N–CH_2–Ar) carbon appeared at 49.2 δ ppm and for alkyl chain in the range 13.7–46.8 δ ppm (see Supplementary 6).

Upon complexation with Ag, two doublets appeared centered at ca. δ188 with Ag–C coupling constants ca. 209 and 181 Hz (see Supplementary 6). These doublets appear in dimeric complexes of structure $[L_2Ag_2]^{2+}$ due to carbene carbon bonding to C–Ag^{107} and C–Ag^{109}, respectively (Baker *et al.,* 2004; Iqbal *et al.,* 2013). In case of Ag–NHC complexes of imidazole neoclide such doublets appear at ca. δ180 with splitting patterns range 180–189 Hz for Ag^{107} and 204–220 Hz for Ag^{109} (Bildstein *et al.,* 1999; Baker *et al.,* 2009). Resonances of aromatic carbons in free ligands (**IV**–**VI**) were found in the comparable region around 113.8–134.5 δ ppm whereas in respective dinuclear complexes (**VII**–**IX**) the observed range is 112.2–136.1 δ ppm. Also, the methylene carbon (N–C–Ar) and alkyl chain

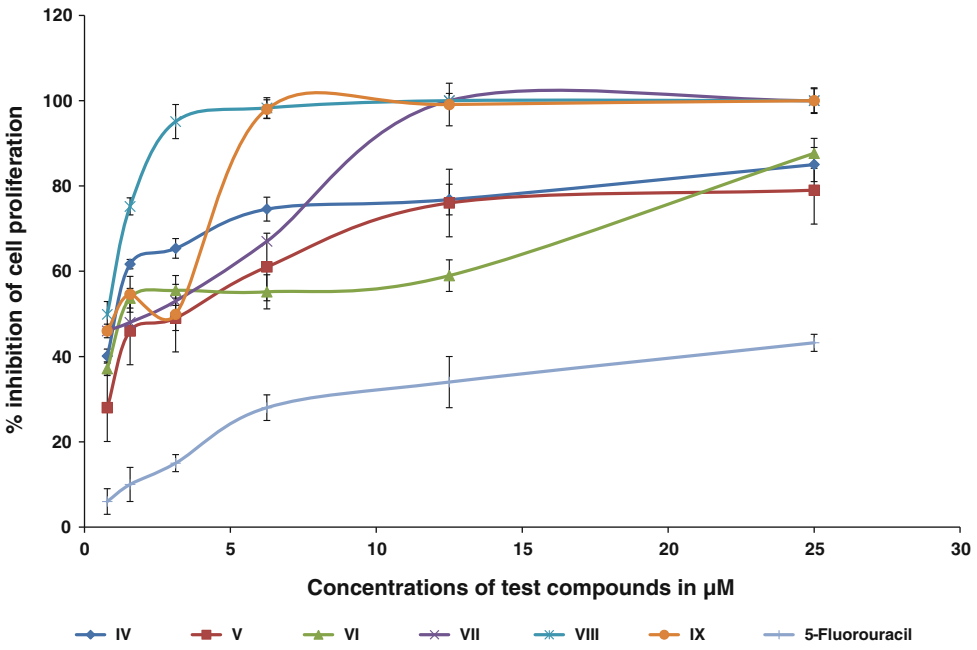

Fig. 3 Dose-dependent anti-proliferative effect of synthetic ligands and their metal complexes on human colorectal tumor cells (HCT 116)

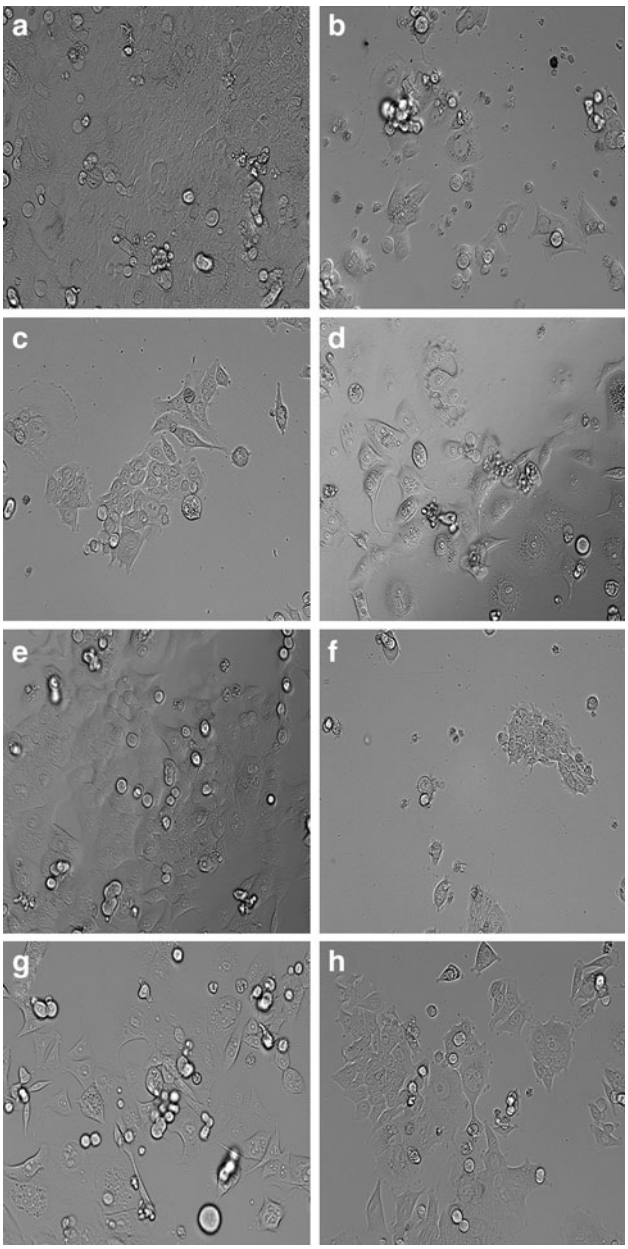

Fig. 4 HCT116 cell images were taken under an inverted phase-contrast microscope at ×200 magnification with a digital camera at 48 h after treatment with the samples. **a** Cells from the control group showed completely intact layer of confluent growth of human colorectal carcinoma (HCT 116) cells. The cells displayed prominent nuclei and cytoplasm. **b** Cells treated with the Standard drug 5-fluorouracil ($IC_{50} = 19.2$ μM). The photomicrograph reveals the obvious cytotoxic effect as evidenced with reduced cell population with weaken cellular morphology. **c** Treatment with **IV**.2Br showed marked inhibition in cell proliferation with $IC_{50} = 0.9$ μM. It can be seen clearly that the population doubling of the cells is reduced drastically after 48 h treatment. The treatment caused severe abrogation of pseudopodial like extensions in cells which rendered the cells to lose their firm surface attachment. **d** Photomicrograph depicts the significant cytotoxic effect of **VII**.$2PF_6$ ($IC_{50} = 2.2$ μM). The picture revealed the clear autophagic characteristic in the cells as all treated cells showed abnormally large number of vacuoles in cytoplasm. **e** Treatment with **V**.2Br showed significant inhibition in cell proliferation with $IC_{50} = 2.8$ μM. The picture revealed the clear signs of toxicity as the cells revealed the abnormal cellular morphology. **f** Photomicrograph showed the effect of treatment with **VIII**.$2PF_6$ exhibited potent inhibition in cell proliferation with $IC_{50} = 0.29$ μM. The picture revealed the affected cell morphology due to the strong cytotoxic effect of the compound. **g** Treatment with **VI**.2Br showed the significant inhibition in cell proliferation. The picture reveals that the cytotoxicity caused by the compound could probably due to the autophagy, as the cells displayed obvious signs of autophagy with clear vacuoles and autophagic bodies in cytosol. **h** Photomicrograph showed that the effect of treatment with **IX**.$2PF_6$ showed marked inhibition in cell proliferation with $IC_{50} = 1.2$ μM. The picture revealed the severely affected cell morphology due to the cytotoxic effect of the compound

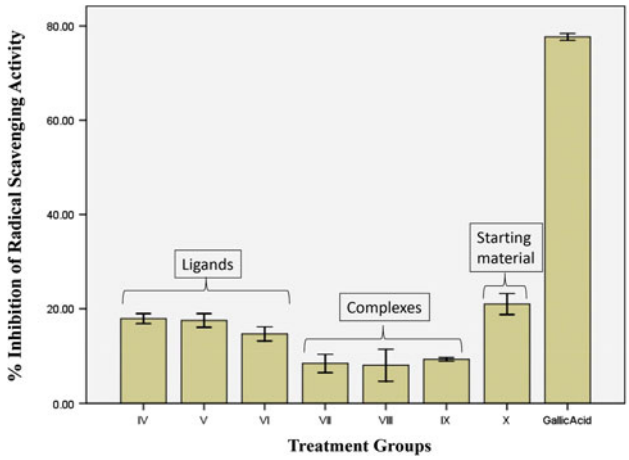

Fig. 5 Comparison between the antioxidant effect of treatment groups and Gallic acid at the maximum used concentration (400 μM)

carbon resonances were observed in the chemical shift regions 51.1 and 13.7–48.7 δ ppm, respectively. These signals are 2–3 δ ppm downfield compared to free ligands (see Supplementary 6).

Table 2 Crystal data and structure refinement details for Ag(I)–NHC complex **VII′**.2PF_6

Formula	$C_{52}H_{52}Ag_2F_{12}N_8P_2$
Formula weight	1294.70
Crystal system	Triclinic
Space group	*P*1
Unit cell dimensions	
a (Å)	9.1620 (5)
b (Å)	11.7393 (7)
c (Å)	13.0947 (8)
α (°)	99.236 (3)
β (°)	107.172 (3)
γ (°)	101.506 (3)
V (Å^3)	1281.87 (13)
Z	1
Density (calcd) (gm/cm^3)	1.677
Abs coeff (mm^{-1})	0.916
F(000)	652
Crystal size (mm)	0.20 × 0.27 × 0.38
Temperature (K)	100
Radiation (Å)	Mo K∝ 0.71073
θ Min, max (°)	1.7, 25.0
Dataset	−10: 10; −13: 13; −15: 15
Tot.; Uniq. Data	4,449
R (int)	0.000
Nref, Npar	4,449, 346
R, wR_2, S	0.0635, 0.2070, 1.05

Table 3 Selected bond lengths (Å) and angles (°) of **VII′**.2PF_6

Bond lengths (Å)					
Ag1–C1	2.083(8)	C26–C25	1.511(12)	N4–C20	1.458(11)
Ag1–C14	2.099(8)	C25–N3	1.464(11)	N3–C15	1.401(11)
C13–C12	1.507(13)	N3–C14	1.359(11)	C15–C20	1.396(11)
C12–N1	1.466(11)	C14–N4	1.353(11)	P1–F1	1.596(6)
N1–C1	1.373(11)	N4–C21	1.458(11)		
C1–N2	1.358(11)	C21–C22	1.517(11)		
Bond angles (°)					
C1–Ag1–C14	171.1(3)		C8–C9–C10	121.1(7)	
C13–C12–N1	111.4(7)		C8–C9–C11	119.9(7)	
C12–N1–C1	124.5(7)		F1–P1–F2	89.8(3)	
N1–C1–N2	104.3(7)		F1–P1–F3	178.8(3)	
C1–N2–C8	124.0(7)				
N2–C8–C9	112.4(6)				

In vitro anti-cancer activity

Effect of benzimidazolium salts (ligands) and their silver complexes on proliferation of HCT 116

In this work, antiproliferative potencies of benzimidazole based ligands and respective dinuclear Ag(I)–NHC complexes were evaluated using MTT assay on cancer cell line, HCT 116. The results were summarized as mean percentage inhibition of cell proliferation (±S.D). All compounds (**IV–IX**) tested against HCT 116 showed more potent antiproliferative activity with IC_{50} (concentration of test substance to achieve 50 % inhibition) in the range 0.9–3.3 μg/ml (Table 1). The results were more pronounced than the standard drug 5-fluorouracil (IC_{50} = 19.2 μM). Recently, we reported anticancer activity of *meta*-xylyl linked bis-benzimidazolium salts (Haque *et al.,* 2012e), where we mentioned that the halide salts of ligands are more active compared to PF_6 salts. We reported same phenomenon for *para*-xylyl linked bis-benzimidazolium salts with *N*-ethyl, propyl, and butyl substitutions (Iqbal *et al.,* 2013), where ligands with chloride counter anions (IC_{50} = 0.3, 1.4 μM) were 17 to 18-fold more active compare to ligand with PF_6 as counter anion (IC_{50} = 18.7 μM) for HCT 116 cell line. It is interesting to notice that the halides are participating in the cytotoxicity against cancer cells. Noticing these results, we now present the synthesis and anticancer activity of similar ligands as bromide salts with *N*-octyl, nonyl, and decyl substitutions. We found interesting results; none of the

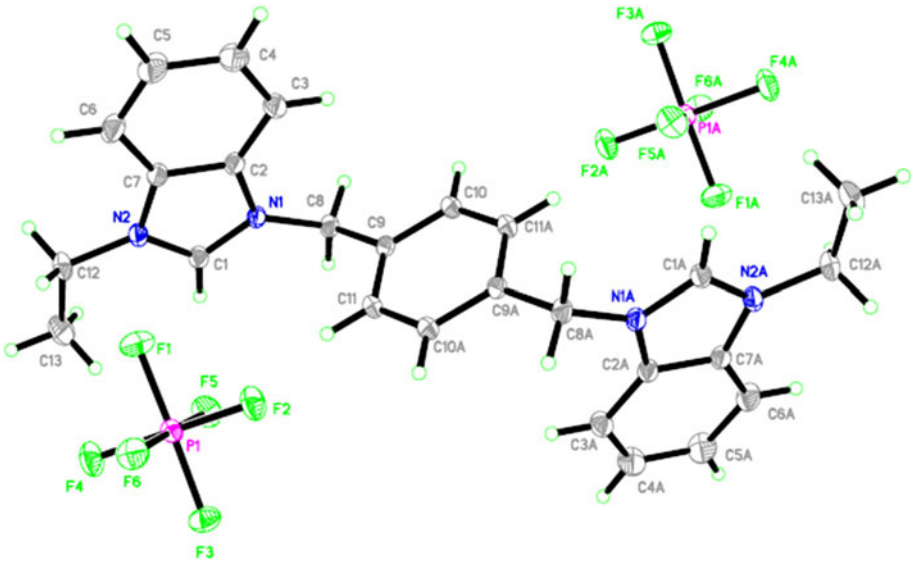

Fig. 6 The ORTEP picture of bis-benzimidazolium salt **IV′**.2PF_6 with displacement ellipsoids drawn at 50 % probability (Iqbal *et al.*, 2013)

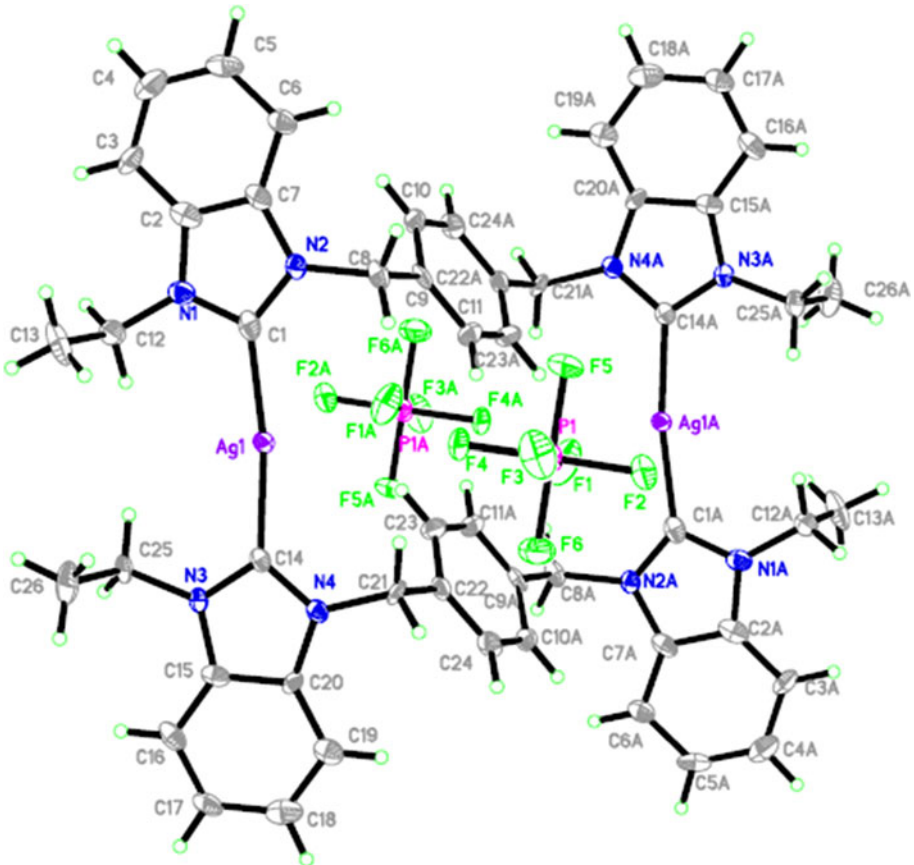

Fig. 7 The ORTEP picture of dinuclear Ag(I)–NHC complex **VII′**.2PF_6 with displacement ellipsoids drawn at 50 % probability

ligands crossed IC_{50} value of 4 μM. The effect of *N*-alkyl substitution is again pronounced i.e., with the increase in size (chain length) of *N*-substitutions, the activity of ligand decreased. However, in respective dinuclear Ag(I)–NHC complexes a reverse occurred. The starting material (**X**, benzimidazole) was also tested against cancer cells and its IC_{50} value was found out to be >200 μg/ml (Table 1). Such a high IC_{50} value for pure benzimidazole also supports significance of halides as counter anions and *N*-alkyl substitutions in bis-benzimidazolium salts.

Figure 3 illustrates the anti-proliferative effect of the test compounds. The graphs clearly show that all the compounds inhibited the proliferation of HCT 116 cells in a dose-dependent manner.

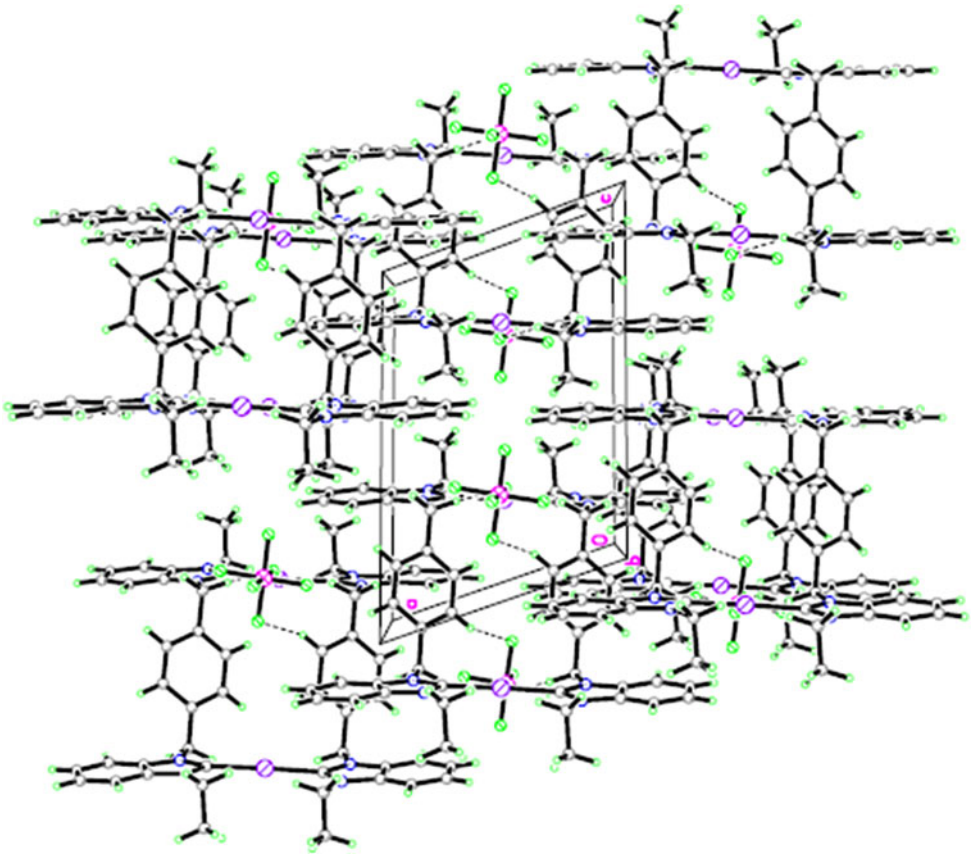

Fig. 8 The ORTEP picture of crystal packing for complex **VII′**.2PF_6

The pure metals are considered to be biologically inactive; however, the activity of metal cations varies on their bioavailability. So delivery methods of metal sources are important parameters to deal metals in biological systems (Kascatan-Nebioglu *et al.,* 2007). The bioavailability of metal cations can be enhanced by connecting them with biologically compatible ligands. Ultimately, the organometallic compounds are generally found to be more active compared to respective organic ligands (Haque *et al.,* 2012a; Iqbal *et al.,* 2013). This has also been one of the conclusions of our studies which narrates that silver in bonding with NHC enhances anticancer activity of bis-benzimidazolium salts. The mechanism of action of silver cations is still not clear to the scientific community; however, the researchers have concluded that silver cations bind to the cell surfaces and interact with enzymes and proteins that are important for cell wall synthesis (Kascatan-Nebioglu *et al.,* 2007). It might also be possible that silver cations on interacting with cell surface affect the cell respiration, metabolism, and transport (Graham, 2005).

The *N*-alkyl substitutions might further affect the potency of the compounds as the substituent produces variation in lipophilicity of the drug. It was found that in case of ligands increase in chain length decreased the anticancer activity for both cell lines; however, in case of respective dinuclear silver (I)–NHC complexes, the activity increased with increase in chain length (see Table 1). However, the values are not as consistent as we reported previously for ethyl-butyl *N*-substitutions (Iqbal *et al.,* 2013). Thus, the anti-proliferative effect of NHCs is probably due to the lipophilicity of the complexes that facilitates the transport of silver cations into the cell and subsequently into the organelles where silver may probably contribute to toxicity by inhibiting cellular respiration and metabolism of biomolecules. Figure 4 shows the cell images of cell line with 48 h control without and with drugs.

Figure 5 shows a comparison between the % inhibition of scavenging activity of treatment groups and positive reference at the maximum used concentration i.e., 400 μM. At a maximum concentration, the % inhibition of Scavenging activity was found to be in the range 6.37–21.00 and 77.68 for drugs **IV**–**X** and Gallic acid, respectively (see Table 1). The results clearly show that the title compounds are not potential antioxidant agents, however; Fig. 5 shows that ligands (**IV**–**VI**) have higher % age inhibition compared to respective Ag(I)–NHC complexes (**VII**–**IX**). This might be due to the presence of acidic proton in ligands at C2 carbon. The acidity due to this proton can be seen in ^{1}H NMR where its peak appears in the range 9.0–10.0 δ ppm (see Supplementary 5), whereas this proton is replaced by silver in respective Ag(I)–NHC complexes which may render to further decrease its activity. In 1974, Cole and coworkers reported that pure benzimidazole and its 2-alkyl

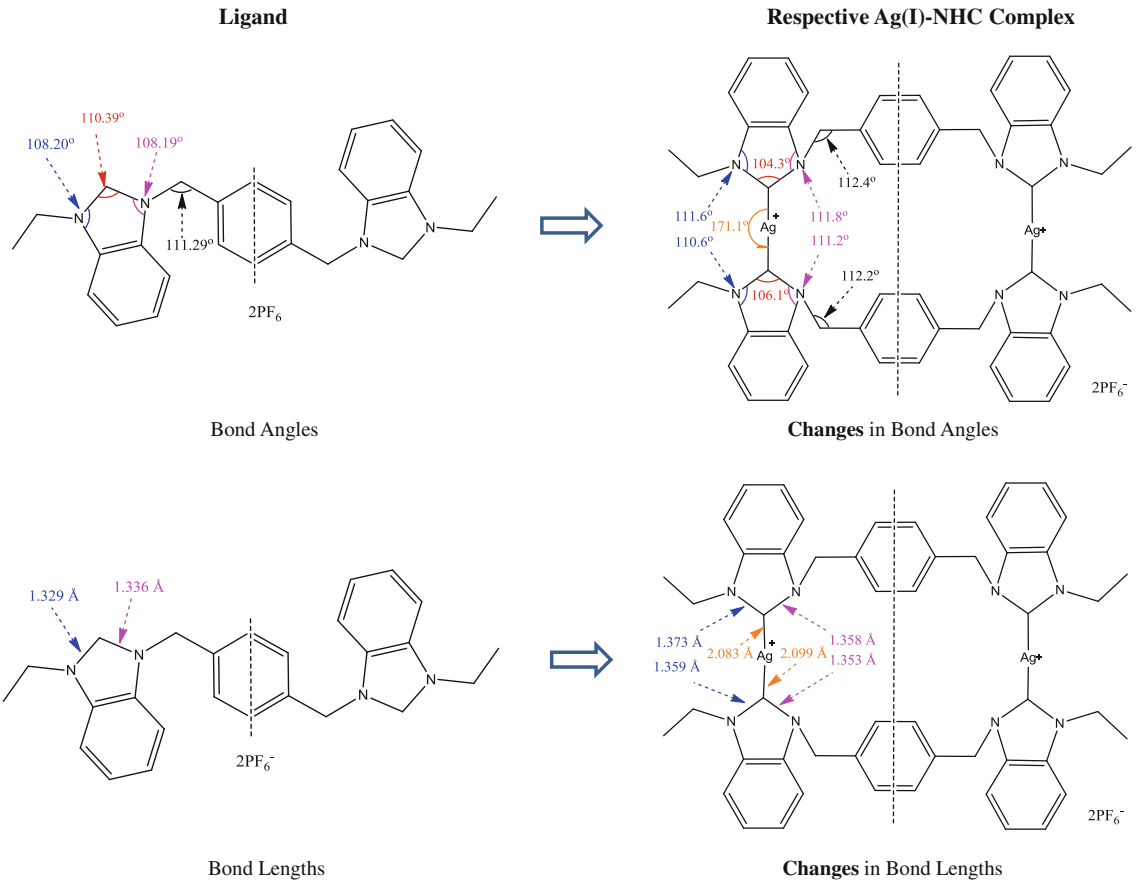

Fig. 9 Comparison of bond angles and bond lengths between ligand **IV**′.2PF_6 and respective dinuclear Ag(I)NHC complex **VII**′.2PF_6. All the labeled values were selected from X-ray crystallographic data. The *figure* clearly shows that after bonding with silver ion, the bond angle at carbene carbon shrinks from 110.39° to 104.30° whereas the bond angles at both *N*-atoms increase from 108.20° to 111.6° ± 0.2°. This shows that the charge density is drifted from imidazolium ring (ligand) to metal ion which causes deviation in *ring shape*. Similarly, significant changes can also be observed in the *C* to *N* bond lengths

derivatives have no direct antioxidant activity (Cole *et al.,* 1974) whereas in 1998, Babizhayev *et al.,* describing structure–activity relationship of imidazole derivatives, mentioned that imidazole ring is responsible for free radical scavenging properties (Babizhayev *et al.,* 1998). However, our results are similar to Cole's findings.

Crystallography

The synthesis, characterization, and anticancer activity of complex "**VII**′.2PF_6" has been described earlier in part-I of this work (Iqbal *et al.,* 2013) where we could not get single crystals suitable for X-ray analysis. However, later on single crystals of title complex were successfully grown by slow evaporation of its saturated solution in a mixture of acetonitrile and water (1:1) at room temperature. Single crystals appeared as colorless blocks. Crystal refinement data, selected bond lengths and angles are tabulated in the Tables 2 and 3. The complex "**VII**′.2PF_6" crystalizes in the triclinic space group P-1 that is the same space group in which respective ligand falls (Iqbal *et al.,* 2013). A perspective view of respective ligand and title complex has been shown in Figs. 6 and 7, respectively. The Fig. 6 shows that the ligand is composed of a bis-benzimidazolium cation and two hexaflourophosphate anions whereas respective dinuclear Ag(I)–NHC complex (Fig. 7) is composed of two ligands sandwiching two silver cations through NHC carbon and two hexflourophosphate anions to neutralize the positive charge of cationic part of the molecule. The benzimidazolyl units found on either side of the central *para*-xylyl core with the dihedral angle 112.2(6). N–C and P–F bond distances are in the range 1.353(11)–1.478(10) and 1.589(6)–1.610(5) Å, respectively. The internal ring angles of benzimidazole (N–C–N) at the carbene center are 104.3(4) for N1–C1–N2 and 106.1(7) for N3–C14–N4. These internal ring angles are 4°–5° smaller in respective silver(I)–NHC complexes than these angles in respective ligand. This is in accordance with the phenomenon that the NHC carbon, after binding with Ag(I) cation, shifts its charge density to metal cation due to

which the shape of imidazole ringe deviates. The comparison of bond distances and angles between ligand and respective dinuclear complex is shown in Fig. 9. The crystal packing (Fig. 8) shows that cationic and anionic components of title salt are connected via C–H–F hydrogen bonding in three-dimensional network.

Conclusions

In conclusion, three new *p*-xylyl linked bis-benzimidazolium salts and their Ag–NHC complexes were synthesized. The compounds were characterized by spectroscopic techniques (FT-IR and NMR) and microanalysis. The single crystals of ligand (**IV′**.2PF_6) and respective complex (**VII′**.2PF_6) were successfully grown and solved by X-ray crystallographic technique. The changes in selected bond lengths and bond angels of ligand and respective metal complex were clearly described by drawing the labeled diagram (Fig. 9). All the compounds were tested for their possible cytotoxicity on human colorectal cancer (HCT 116) and antioxidant evaluation. All tested compounds showed dose-dependent cytotoxicity against human colon cancer. The IC_{50} values for HCT 116 cells range between 0.29 and 3.30 μM which is significantly better than commercially available drug (5-FU, IC_{50} = 19.2 μM). Among all, the complex **VIII**.2PF_6 was found to be the most active against human cancer cell line (IC_{50} = 0.29 μM). Based on the results it can be concluded that dinuclear Ag(I)–NHC complexes of bis-benzimidazolium salts could probably be the potential source of chemotherapeutic drugs. Due to encouraging results, further study on these complexes is in progress.

Acknowledgments RAH thanks Universiti Sains Malaysia (USM) for the Research University (RU) Grants (1001/PKIMIA/811157) and (1001/PKIMIA/823082). MAI is grateful to (IPS) USM for financial support [fellowship: USM.IPS/JWT/1/19 (JLD 6): P-KD0030/11(R)] and funds [P-KM0018/10(R)-308/AIPS/415401] for a research attachment (Aug. 2011–Nov. 2011) to University of Western Australia (UWA), Perth, Australia.

References

Babizhayev M, Courbebaisse Y, Nicolay J-F, Semiletov Y (1998) Design and biological activity of imidazole-containing peptidomimetics with a broad-spectrum antioxidant activity. Lett Pept Sci 5(2–3):163–169

Baker MV, Brown DH, Haque RA, Skelton BW, White AH (2004) Dinuclear *N*-heterocyclic carbene complexes of silver(i), derived from imidazolium-linked cyclophanes. Dalton Trans 21: 3756–3764

Baker MV, Brown DH, Haque RA, Skelton BW, White AH (2009) Silver(I) and mercury(II) complexes of *meta*- and *para*-xylyl linked bis(imidazol-2-ylidenes). J Incl Phenom Macrocycl Chem 65(1):97–109

Bansal Y, Silakari O (2012) The therapeutic journey of benzimidazoles: a review. Bioorg Med Chem 20(21):6208–6236

Bildstein B, Malaun M, Kopacka H, Wurst K, Mitterböck M, Ongania K-H, Opromolla G, Zanello P (1999) *N*, *N′*-Diferrocenyl-*N*-heterocyclic carbenes and their derivatives. Organometallics 18(21):4325–4336

Cole ER, Crank G, Salam-Sheikh A (1974) Antioxidant properties of benzimidazoles. J Agric Food Chem 22(5):918

Graham C (2005) The role of silver in wound healing. Br J Nutr 14(19):S22

Haque RA, Iqbal MA (2012a) Synthesis and characterization of *ortho*-xylyl linked bis-benzimidazolium salts. Asian J Chem 24(6):2625–2628

Haque RA, Iqbal MA (2012b) Synthesis and characterization of *ortho*-xylyl linked bis-benzimidazolium salts (Part-II). Asian J Chem 25(4):3049–3054

Haque RA, Iqbal MA, Hemamalini M, Fun H-K (2011) 3,3′-[1,2-Phenylenebis(methylene)]bis(1-heptylbenzimidazolium) dibromide monohydrate. Acta Crystallogr E 67(7):o1814–o1815

Haque RA, Ghdhayeb MZ, Budagumpi S, Salman AW, Khadeer Ahamed MB, Majid AMSA (2012a) Non-symmetrically substituted N-heterocyclic carbene–Ag(I) complexes of benzimidazol-2-ylidenes: synthesis, crystal structures, anticancer activity and transmetallation studies. Inorg Chim Acta 392:61–72

Haque RA, Iqbal MA, Ahmad SA, Chia TS, Fun H-K (2012b) 3,3′-[1,4-Phenylenebis(methylene)]bis(1-propylbenzimidazolium) dichloride dihydrate. Acta Crystallogr E 68(3):o845–o846

Haque RA, Iqbal MA, Budagumpi S, Hemamalini M, Fun H-K (2012c) 3,3′-[1,2-Phenylenebis(methylene)]bis(1-ethylbenzimidazolium) dibromide. Acta Crystallogr E 68(3):o573

Haque RA, Iqbal MA, Fun H-K, Arshad S (2012d) 3,3′-[1,2-Phenylenebis(methylene)]bis(1-octylbenzimidazolium) dibromide monohydrate. Acta Crystallogr E 68(4):o924–o925

Haque RA, Iqbal MA, Khadeer MB, Majeed AA, Abdul Hameed ZA (2012e) Design, synthesis and structural studies of *meta*-xylyl linked bis-benzimidazolium salts: potential anticancer agents against 'human colon cancer'. Chem Cent J 6(1):68

Haque RA, Iqbal MA, Rosli MM, Fun H-K (2012f) 3,3′-[1,2-Phenylenebis(methylene)]bis(1-ethyl-1H-benzimidazol-1-ium) bis(hexaflourophosphate). Acta Crystallogr E 68(6):o1635

Hranjec M, Starčević K, Pavelić SK, Lučin P, Pavelić K, Karminski Zamola G (2011) Synthesis, spectroscopic characterization and antiproliferative evaluation in vitro of novel Schiff bases related to benzimidazoles. Eur J Med Chem 46(6):2274–2279

Iqbal MA, Haque RA, Ahamed MBK, Abdul MAMS, Al-Rawi S (2013) Synthesis and anticancer activity of *para*-xylyl linked bis-benzimidazolium salts and respective Ag(I) *N*-heterocyclic carbene complexes. Med Chem Res. doi:10.1007/s00044-00012-00240-00046

Kascatan-Nebioglu A, Panzner MJ, Tessier CA, Cannon CL, Youngs WJ (2007) *N*-Heterocyclic carbene-silver complexes: a new class of antibiotics. Coord Chem Rev 251(5–6):884–895

Kim KS, Lee S, Lee YS, Jung SH, Park Y, Shin KH, Kim B-K (2003) Anti-oxidant activities of the extracts from the herbs of Artemisia apiacea. J Ethnopharmacol 85(1):69–72

Narasimhan B, Sharma D, Kumar P (2012) Benzimidazole: a medicinally important heterocyclic moiety. Med Chem Res 21(3):269–283

Starikova OV, Dolgushin GV, Larina LI, Ushakov PE, Komarova TN, Lopyrev TN (2003) Synthesis of 1,3-dialkylimidazolium and 1,3-dialkylbenzimidazolium salts. Russ J Org Chem 39(10): 1467–1470

Weitz J, Koch M, Debus J, Höhler T, Galle PR, Büchler MW (2005) Colorectal cancer. The Lancet 365(9454):153–165